ESOMAT 2009, 02036 (2009)
DOI:10.1051/esomat/200902036

In-situ TEM study of stress-induced transformations in CuAlNi

N. Zárubová[a], J. Gemperlová, A. Gemperle, Z. Dlabáček

Institute of Physics, ASCR v.v.i., Na Slovance 2, 182 21 Prague 8, Czech Republic

Abstract. Stress-induced martensitic transformations and twinning processes were studied in thin foils of CuAlNi single crystals strained *in-situ* in a transmission electron microscope. A detailed structure analysis comprised identification of phases existing under stress and determination of their mutual crystallographic orientation. Three transformation processes were detected: i) transformation of austenite into 2H martensite at low stress levels; ii) twinning/detwinning processes in 2H martensite, and iii) transformation between austenite and 18R martensite at higher stress levels. Nucleation and growth of martensite plates were followed, and morphology of the austenite/martensite habit planes was examined. Existence of planar interfaces between a single variant of 2H martensite and austenite on microscopic level was proved.

1. Introduction

Cu-base alloys are attractive for fundamental research of the thermo-mechanical properties of shape memory materials (superelasticity, shape memory effect, twinning in martensite) because the martensitic transformations in them are fairly well known and the related deformation processes are linked with large reversible strains. Besides, Cu-base alloys can be relatively easily prepared in the form of oriented single crystals.

In CuAlNi alloys subjected to stress-free cooling, the $D0_3$ ordered parent phase (β_1 austenite) transforms into orthorhombic 2H (γ_1') or monoclinic 18R (β_1') martensite, or into a mixture of both, depending on the alloy composition [1]. In the presence of an external stress, multistage thermoelastic behavior is observed reflecting variety of successive austenite-to-martensite and martensite-to-martensite transitions [2-6]. Beside γ_1' and β_1' martensites, also α_1' (monoclinic 6R) structure was reported in CuAlNi single crystals subjected to tensile stress in the $[100]_{\beta 1}$ direction [4,6]. *In-situ* light microscopy and X-ray diffraction were utilized to follow the morphological changes associated with successive martensitic transformations under stress and the resulting crystal structures [2-4]. *In-situ* observations by light microscopy were also successfully used on CuAlNi and CuAlMn single crystals to monitor the austenite-martensite interface propagating under tensile [7] or compression [8,9] straining. The crystal structure, internal defects, habit planes and orientation relationships of the stress-induced γ_1' and β_1'martensites were comprehensively investigated by transmission electron microscopy (TEM) in [10,11]. The analysis, however, was made *ex-situ* on stress-induced martensites in the unstressed state. In order to obtain a closer insight into the dynamically evolving microstructures, *in-situ* TEM straining experiments seem to be a very suitable technique [12-16].

2. Experimental

A single crystal of nominal composition Cu-13.9Al-4.4Ni (in wt. %) grown by the Bridgman technique was used for the experiment. The as-grown crystal (80mm long, 22 mm in diameter) was annealed at 950°C for 1 hour in Ar atmosphere and quenched into a mixture of ice and water. The resulting structure at room temperature was β_1 ($D0_3$) austenite. The transformation temperatures estimated by calorimetry were approximately M_S = -27°C, A_f = +20°C indicating $\beta_1 \leftrightarrow \gamma_1$' transformation in the thermal cycle.

Tensile samples 1.7 x 5.5 x 0.07 mm^3 thinned to electron transparency in the central part [16] were used for the TEM straining. The foil surface was close to $(\bar{1}\,2\,0)_{\beta 1}$ plane, the longitudinal axis close to $[6\,3\,\bar{2}]_{\beta 1}$ direction (see Fig.1). The samples were strained in tension at room temperature in a JEM 1200EX microscope equipped with a double tilt straining stage (x-tilt ± 30°, y-tilt ± 10°, load max. 25 N) designed and constructed

[a] e-mail: zarubova@fzu.cz

Article available at http://www.esomat.org or http://dx.doi.org/10.1051/esomat/200902036

at the Institute of Physics ASCR [17]. Only the load was measured during straining, the elongation was not registered. The highest load, F, applied in the experiments was about 12 N. The transformation processes were recorded during loading and unloading by a Mega View III camera. Detailed structural observations were made under stress in two-beam conditions both in bright and dark fields.

3. Results

The observations described below were made in the proximity of the places where the tangent to the hole was parallel to the longitudinal specimen axis. The axis of the major principal stress (local tensile axis) in the material remains parallel to the external tensile axis at those places and the magnitude of the stress is the highest there [18,19]. From the calculations performed in Ref. [18] we can estimate that a load of 1 N corresponds to an average tensile stress of about 130 MPa in the regions of observation.

The lattice correspondence between the martensites (M) and the parent β_1 phase was supposed to be $[100]_M$ // $<110>_{\beta 1}$, $[010]_M$ // $<100>_{\beta 1}$, $[001]_M$ // $<110>_{\beta 1}$, in agreement with [10,11]. This relationship gives six variants for γ_1' martensite and 12 variants for β_1' and α_1' martensites. The lattice correspondences of variants V1 to V6' were defined as given in Table 1. The diffraction patterns from individual martensitic needles were fitted to β_1'(18R), γ_1' (2H) and α_1'(6R) structures with the requirement that the solution satisfy (with an accuracy of 10 deg) one of the martensite-austenite lattice correspondences in Table 1. The lattice parameters and atomic arrangements of β_1', γ_1'and α_1' structures were taken from Ref. [20]; a_o = 0.5835 nm were used for the cubic β_1 austenite [8]. Up to three different diffraction patterns from the same martensite plate, acquired by tilting the straining stage, were necessary to identify the structure and the orientation of the plate unambiguously. Identification of martensite variants is described in detail in our previous paper [16].

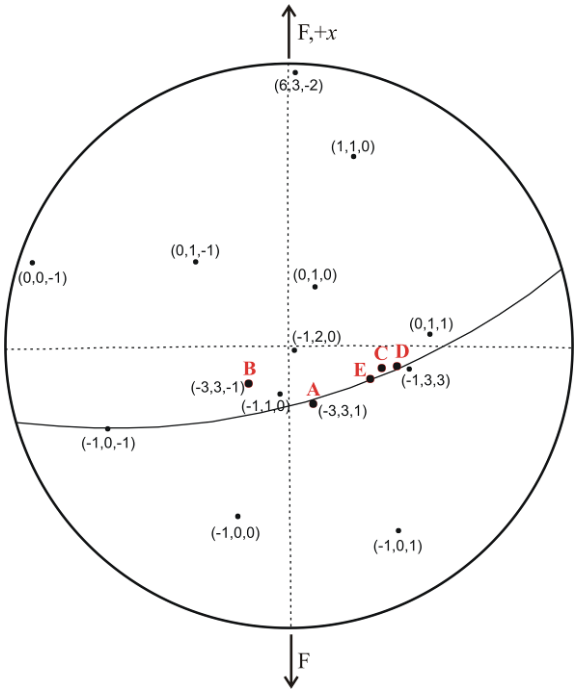

Fig. 1. Stereographic projection of the foil in β_1 austenite state. F, +*x* – direction of the external load and the +*x* tilt axis. A, E,C, D – normals to β_1/γ_1'(V3) interfaces; B – normal to β_1/γ_1'(V1) interface

Table 1. Lattice correspondences between β_1 austenite and martensites. M stands for α_1', β_1' and γ_1'. Variants V1, V1', etc. are identical for γ_1' martensite.

	$[100]_M$	$[010]_M$	$[001]_M$
V1	$[0\,\bar{1}\,1]_{\beta_1}$	$[100]_{\beta_1}$	$[011]_{\beta_1}$
V1'	$[01\bar{1}]_{\beta_1}$	$[\bar{1}00]_{\beta_1}$	$[011]_{\beta_1}$
V2	$[011]_{\beta_1}$	$[100]_{\beta_1}$	$[01\bar{1}]_{\beta_1}$
V2'	$[0\bar{1}\,\bar{1}]_{\beta_1}$	$[\bar{1}00]_{\beta_1}$	$[01\bar{1}]_{\beta_1}$
V3	$[10\bar{1}]_{\beta_1}$	$[010]_{\beta_1}$	$[101]_{\beta_1}$
V3'	$[\bar{1}01]_{\beta_1}$	$[0\bar{1}0]_{\beta_1}$	$[101]_{\beta_1}$
V4	$[101]_{\beta_1}$	$[010]_{\beta_1}$	$[\bar{1}01]_{\beta_1}$
V4'	$[\bar{1}\,0\,\bar{1}]_{\beta_1}$	$[0\bar{1}0]_{\beta_1}$	$[\bar{1}01]_{\beta_1}$
V5	$[\bar{1}\,10]_{\beta_1}$	$[001]_{\beta_1}$	$[110]_{\beta_1}$
V5'	$[1\,\bar{1}\,0]_{\beta_1}$	$[00\bar{1}]_{\beta_1}$	$[110]_{\beta_1}$
V6	$[110]_{\beta_1}$	$[001]_{\beta_1}$	$[1\,\bar{1}\,0]_{\beta_1}$
V6'	$[\bar{1}\,\bar{1}\,0]_{\beta_1}$	$[00\bar{1}]_{\beta_1}$	$[1\,\bar{1}\,0]_{\beta_1}$

The first martensite needles appeared at the hole edge (Fig. 2) at loads of about 0.7 N (local tensile stress ≈ 100 N [18]). They were identified as variants V3 of γ_1' martensite. With increasing stress, the γ_1'(V3) needles grew extremely rapidly to their final size (no details of the $\beta_1 \rightarrow \gamma_1$' transformation process could be video-recorded), reaching dimensions of about 10 μm in some cases. No reverse γ_1' → β_1 transformation took place under unloading. In the thinnest areas of the foil, near the hole edge, the γ_1' martensite needles consisted of a single variant with a smooth γ_1'/ β_1 habit plane (see the upper part of the γ_1'(V3) martensite needle in Fig. 2).

In thicker areas of the foil, the γ_1' martensite was twinned. It is apparent in the lower part of the γ_1'(V3) needle in Fig. 2 (marked by black arrows). Fig. 3 shows in detail the boundary between a large γ_1'(V3) plate and the β_1 austenite. The wedge shaped needles, identified as γ_1'(V1) variant, are surrounded by γ_1'(V3) variant that forms the rest of the martensite plate. The habit plane between austenite and γ_1' martensite is of zig-zag shape and consists of two types of differently oriented facets. The facets larger than 1 μm were observed in some cases. The crystallography of the facets forming the β_1 / γ_1' habit plane in Fig. 3 was determined by stereo-microscopy [21]. Facet A, the interface between γ_1'(V3) and β_1, was found very close to $(\bar{3}\,3\,1)_{\beta 1}$ plane while facet B, between γ_1'(V1) and β_1, was identified as $(\bar{3}\,3\,\bar{1})_{\beta 1}$ plane. However, different crystallographic planes were found for other γ_1'(V3) / β_1 interfaces (see Fig. 1).

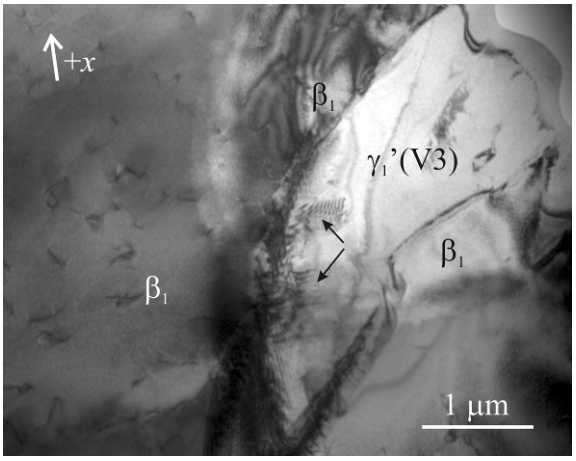

Fig. 2. γ_1'(V3) martensite needle which nucleated at the hole edge at a load of 0.8 N. The black arrows mark twins in the γ_1'(V3) variant. F = 3 N, DF $202_{\beta 1}$

White arrow indicates +*x* tilt axis.

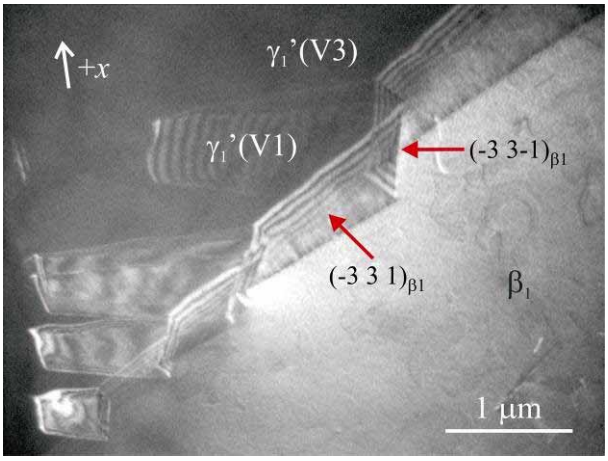

Fig. 3. Habit plane between β_1 austenite and twinned γ_1' martensite. The boundary is formed by segments of two $\{3\,3\,1\}_{\beta 1}$ planes (marked by red arrows). F = 2 N, DF $202_{\beta 1}$

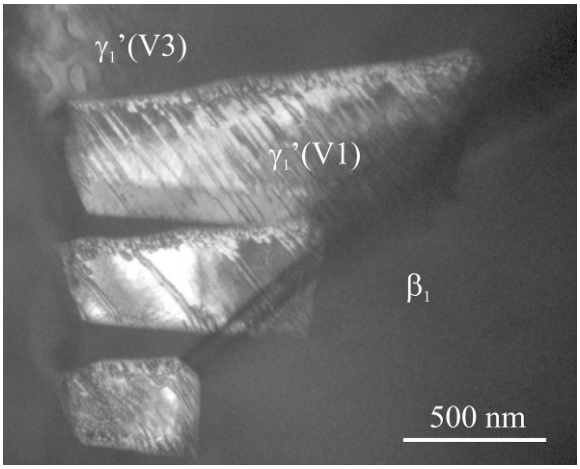

Fig. 4. Structural defects in γ_1' martensite. Enlarged area of the left lower corner of Fig. 3. F = 5.2 N, DF $201_{\gamma 1'}$

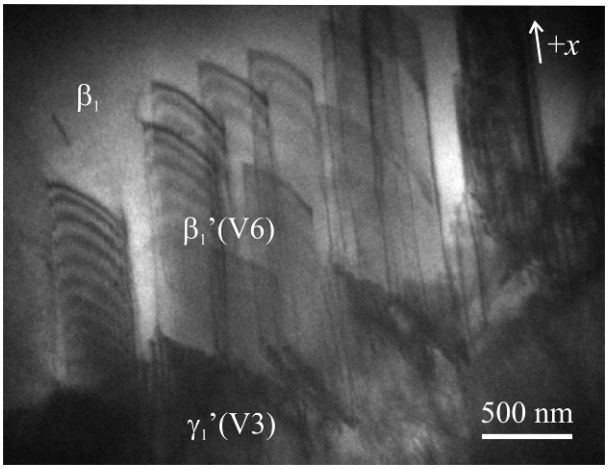

Fig. 5. Transformation β_1 austenite ↔ β_1' martensite. The β_1'(V6) variant nucleated at an γ_1' martensite needle. F = 7 N, a frame of video-record.

With increasing load, the γ_1'(V1) needles stepwise disappeared being replaced by the more favorably oriented variant γ_1'(V3). During unloading, the γ_1'(V1) needles grew back in their original shapes [16]. The twin planes between variants γ_1'(V1) and γ_1'(V3), determined by the stereo-microscopy [21], were situated near the $(\bar{1}\,2\,\bar{1})_{\gamma 1'}$ plane of variant γ_1'(V3), i.e. near $(\bar{1}\,1\,0)_{\beta 1}$ plane in the austenite. The combination of variants γ_1'(V3)

and γ_1'(V1) represents thus type I twinning. Pronounced structural defects are clearly visible in γ_1'(V1) martensite needles under suitable imaging conditions (Fig. 4). Similar defects were not found in the variant γ_1'(V3), which suggests that the defects are located in the γ_1'(V1) / γ_1'(V3) twin plane. Their nature is, however, not yet clear.

At loads of about 2 N (tensile stresses of ≈ 260 MPa), the first β_1'martensite needles were detected. The β_1' needles nucleated always at the already existing γ_1' martensite as documented in Fig. 5. The β_1' plates were identified predominantly as β_1'(V3) or β_1'(V6) variants. The β_1' needles developed in the number and length with increasing load and grew by a jerky movement of the needle tip. During unloading, the β_1' needles transformed back into the β_1 matrix. Unlike the γ_1' martensite, the propagation of the β_1' martensite needles under stress could be easily video-recorded.

4. Discussion

Let us compare briefly the transformation behavior of strained thin foils with the transformation responses of bulk single crystals, expressed conventionally in the form of σ-T phase diagrams [2,4-6]. We shall compare our observations with the results by Otsuka et al [2] who tensile strained CuAlNi single crystals of a composition and orientation very similar to our foils. The test temperature in our TEM straining experiments was in the close proximity of A_f (≈ +20°C). According to the σ-T diagram shown in Fig. 11 in [2], formation of γ_1' and β_1' martensites at low stress levels should be expected with the same probability. However, the stress-induced transformation in the foils started always with formation of γ_1' martensite. The rough estimate of the stress at which the first γ_1' needles appeared is about 100 N, in good agreement with macroscopic measurements [2,5]. Once the γ_1' needle had nucleated, it spread extremely rapidly to its final dimension. The $\beta_1 \rightarrow \gamma_1$' transformation in the thin foil seems to correspond well to the macroscopic observation of a sharp peak at the beginning on the stress-strain curve connected with formation of the first band of γ_1' martensite [2]. On the other hand, formation of β_1' martensite is obviously more difficult in the thin foil, and the first β_1' needles appear at higher stresses than the γ_1' ones. The complicated boundaries between the already existing γ_1' martensite and the parent austenite (Fig. 3) serve as sites of preferential nucleation of β_1' martensite, probably because of their crystallographic geometry. Nucleation of 18R martensite on the tip of a 2H martensite needle during *in-situ* TEM straining experiments was described also in CuAlMn alloy [13].

An interesting feature of the structural observations in the strained foils is the morphology of the γ_1' martensite. In the thinnest areas close to the hole, the γ_1' plates were formed by one variant (V3), no twins were discernible and the γ_1'/ β_1 boundary was smooth (see the upper part of the γ_1'(V3) needle in Fig.2). According to the crystallographic theory of martensite [22], there is no solution for a planar interface between the austenite and a single variant of γ_1' martensite (so called *exact* interface) in bulk CuAlNi. However, an *exact* γ_1'/ β_1 interface can be formed under specific conditions in a thin film [22]. Ostapovets [23] analyzed these conditions for the case of our CuAlNi foils. He found that in the foil with the surface normal strictly $[\,\bar{1}\,2\,0\,]_{\beta 1}$, an *exact* interface between β_1 austenite and γ_1' (V3) martensite variant cannot form. Nevertheless, for a deviation of about 6° (and more) from $[\,\bar{1}\,2\,0\,]_{\beta 1}$ the conditions for existence of an *exact* γ_1'(V3)/β_1 interface can be fulfilled. This may explain the morphology of the γ_1' plates and the smooth γ_1'/ β_1 habit plane observed near the hole. The strained foil behaves as a thin film there.

In a greater distance from the hole where the foil was thicker, the γ_1' martensite was twinned (Figs. 3) consisting of variants γ_1'(V3) and γ_1'(V1). This combination represents type I twinning as follows from the measured twin planes near $(\,\bar{1}\,2\,\bar{1}\,)_{\gamma 1=}$. The morphology of the γ_1'/ β_1 boundary shown in Fig. 3 demonstrates that planar interfaces between austenite and a single martensite variant can exist on the microscopic level. As described in [23] the habit plane crystallography depicted in Fig. 3 can be no more explained in the frame of 2-dimensional (thin film) phenomenological theory and must be treated as a 3-dimentional case [24, 25]. Since no "additional" twins could be detected in the vicinity of the $\{331\}_{\beta 1}$ segments, a simple shear was taken as a lattice-invariant deformation in the model. The nature of the simple shear is being examined at present. However, preliminary results [25] indicate that it might be related to the structural defects observed in γ_1' martensite (Fig. 4).

4. Conclusions

The strain-induced transformation processes in thin foils correspond well to the austenite ↔ martensite transformations described in bulk specimens. However, nucleation of 18R martensite is more difficult than nucleation of 2H martensite in the thin foil. Relatively long smooth interfaces form between austenite and a single variant of 2H martensite. The existence of these *exact* γ_1'/β_1 interfaces can be explained on the base of the phenomenological theory of martensitic transformation.

The authors highly acknowledge the financial support of the Grant Agency of ASCR (contract No. A200100627).

References

[1] H. Warlimont, L. Delaey, Progress in Material Science **18**, 1 (1974)
[2] K. Otsuka, C.M. Wayman, K. Nakai, H. Sakamoto, K. Shimizu, Acta Metall. **24**, 207 (1976)
[3] C. Rodriguez, L.C. Brown, Metallurgical Trans. **7A**, 265 (1976)
[4] K. Otsuka, H. Sakamoto, K Shimizu, Acta Metall. **27**, 585 (1979)
[5] V. Novák, J. Malimánek, N. Zárubová, Mater. Sci. Eng. A **191**, 193 (1995)
[6] V. Novak, P. Sittner, J. van Humbeeck, J. Phys. IV **11**, Pr8-191 (2001)
[7] T. W. Shield, J. Mech, Phys. Solids **43**, 869 (1995)
[8] V. Novák, P. Šittner, S. Ignacová, T. Černoch, Mater. Sci. Eng. A **438-440**, 755 (2006)
[9] S. Ignacová, T. Černoch, V. Novák, P. Šittner, Mater. Sci. Eng. A **481-482**, 526 (2008)
[10] K. Otsuka, T. Nakamura, K. Shimizu, Trans. JIM **15**, 200 (1974)
[11] K. Otsuka, T. Nakamura, K. Shimizu, Trans. JIM **15**, 211 (1974)
[12] J. Stoiber, R. Gotthart, Mater. Sci. Eng. A **164**, 443 (1993)
[13] J. Dutkiewicz, H. Kato, S. Miura, U. Messerschmidt, M. Bartsch, Acta Mater. **44**, 4597 (1996)
[14] A. Ibarra, J. San Juan, E.H. Bocanegra, D. Caillard, M.L. Nó, Mater. Sci. Eng. A **438-440**, 787 (2006)
[15] A. Ibarra, D. Caillard, J. San Juan, M.L. Nó, Applied Phys. Letters **90**, 101907 (2007)
[16] N. Zárubová, J. Gemperlová, V. Gärtnerová, A. Gemperle, Mater. Sci. Eng. A **481-482**, 457 (2008)
[17] Z. Dlabáček, A. Gemperle, J. Gemperlová, "Improved design of a double tilt side entry straining stage for TEM", 13th European Microscopy Congress, Antwerp 2004, edited by D. Schryvers and J.-P. Timmermans, p. 417
[18] A. Coujou, Ph. Lours, N.A. Roy, D. Caillard, N. Clement, Acta Metall. **38**, 825 (1990)
[19] N. Zárubová, A. Gemperle, J. Gemperlová, Mater. Sci. Eng. A **462**, 407 (2007)
[20] K. Otsuka, T. Ohba, M. Tokonami, C. M. Wayman, Scripta Metal. Mater. **29,** 1359 (1993)
[21] J.F. Nankiwell, Optik **20**, 171 (1963)
[22] K. Bhattacharya, *Microstructure of Martensite* (Oxford University Press, Oxford, 2003)
[23] A. Ostapovets, Ph.D. Thesis, Prague 2009
[24] A. Ostapovets, V. Paidar, N. Zarubova, Int. J. Mat. Res. (formerly Z. Metallkd.) **100**, 342 (2009)
[25] A. Ostapovets, V. Paidar, N. Zarubova, "Cu-Al-Ni microstructure in the phenomenological theory of martensite with lattice invariant deformation", ESOMAT2009, Prague 2009